SPECTRAL CLASSIFICATION OF SIMILAR MATERIALS USING THE TETRACORDER ALGORITHM: THE CALCITE-EPIDOTE-CHLORITE PROBLEM

J. Brad Dalton,[1] Dana Bove,[2] Carol Mladinich,[2] Roger Clark,[2] Barnaby Rockwell,[2] Gregg Swayze,[2] Trude King,[2] and Stanley Church[2]

1. INTRODUCTION

Recent work on automated spectral classification algorithms has sought to distinguish ever-more similar materials. From modest beginnings separating shade, soil, rock and vegetation (Soha *et al*., 1976) to ambitious attempts to discriminate mineral types (Kruse *et al*., 1993; Boardman, 1993; Clark and Swayze, 1995) and specific plant species (Kokaly *et al*., 1997), the trend seems to be toward using increasingly subtle spectral differences to perform the classification. Rule-based expert systems exploiting the underlying physics of spectroscopy such as the USGS Tetracorder system (Clark *et al*., 2001) are now taking advantage of the high spectral resolution and dimensionality of current imaging spectrometer designs (*cf*. Eastwood *et al*., 2000) to discriminate spectrally similar materials. The current paper details recent efforts to discriminate three minerals having absorptions centered at the same wavelength, with encouraging results.

2. THE CALCITE-EPIDOTE-CHLORITE PROBLEM

2.1 Relevance

One of the applications of remote hyperspectral analysis is the examination of mineralogy in mining districts. The current study was undertaken as part of the Animas River Watershed study (Nimick and von Guerard, 1998) of the U.S. Geological Survey Abandoned Mine Lands (AML) Project. A key goal of this project is the determination of levels of acidic mine drainage in the watershed, which includes several hydrothermal alteration zones (Bove *et al*., 2000) associated with the Silverton Caldera in the San Juan Mountains of southwestern Colorado. Weathering of pyrite (FeS_2) results in an assemblage of minerals, which includes goethite, hematite and jarosite (Bigham *et al*., 1996), as well as production of sulfuric acid (H_2SO_4) which then contaminates runoff, usually acquiring a load of dissolved metals along the way (Mast *et al*., 2000) and eventually enters the river. In the Silverton Caldera, large areas of naturally-occurring exposed hydrothermal alteration zones (*ibid*.) contribute significant quantities of acid to the watershed, complicating efforts to ascertain the level of anthropogenic impact.

The Silverton Caldera overlies preexisting sedimentary rock containing large quantities of calcite as limestone (Lipman *et al*., 1973). Where the acidic waters combine with waters that have passed through these limestone beds, the buffering action of the carbonates reduces the acidity of the water. This has strong effects on the water quality and concentrations of dissolved metals (Church *et al*., 2000). Calcite also occurs within the igneous rock, at much lower concentrations, as a result of propylitic alteration. In order to accurately assess and model effects of pyrite weathering from natural and artificial sources, land managers and aqueous geochemists need to determine the occurrence and distribution of calcite in the watershed.

Previous attempts to classify and map calcite through hyperspectral imagery (Dalton *et al*., 1998, 2000) have been held up by the spectral similarity of calcite to both epidote and chlorite, which also result from propylitic alteration. In such alteration zones, these three minerals are typically found together as a fine-grained mixture that appears homogeneous at greater than centimeter scales, but may be readily distinguished by field geologists upon examination with a hand-lens or microscope. Chlorite may have weak buffering capabilities (DesBorough *et al*., 1998), though these are an order of magnitude weaker than those of calcite. A determination of stream buffering

[1] NASA-Ames Research Center, Mountain View, California 94035 (dalton@mail.arc.nasa.gov)
[2] U.S. Geological Survey, Denver, Colorado 80225

capacity in the watershed therefore requires knowledge of the distribution and abundance of all three minerals. Thus, solving the Calcite-Epidote-Chlorite problem became a primary interest for the authors of this study.

2.2 Spectral Comparisons

Near-infrared spectra of calcite, epidote and chlorite in the 2.0- to 2.5-μm (micron) range are shown in Figure 1. The diagnostic infrared absorption band of calcite ($CaCO_3$) is centered at 2.34 μm, as are those of epidote ($Ca_2(Fe^{3+},Al)_3(SiO_4)_3(OH)$) and chlorite ($(Mg,Fe^{2+})_5Al(Si_3Al)O_{10}(OH)_8$). Although chlorite is actually a broad term referring to a large family of minerals (Klein and Hurlbut, 1993), in this study we refer to a specific chlorite, ripidolite, which is a ferroan clinochlore (Fleischer and Mandarino, 1995) and is the primary type found in the study area. The 2.3 μm chlorite band complex may vary its shape, intensity and position in response to changes in composition (Hunt and Salisbury, 1970; King and Clark, 1989), and so care is recommended in applying the results of this study to other locations. The secondary band at 2.26 μm in the chlorite spectrum, for example, may change in strength relative to the primary band at 2.34 μm. However, for pure samples of the chlorite used in this study, the band positions and relative strengths remained constant with respect to grain size, as they did for the epidote. There is no corresponding band in the calcite spectrum, although a small shoulder is seen in the primary absorption band at 2.3 μm. Calcite does feature a weak absorption at 2.15 μm, which is not seen in the other two minerals. Finally, an absorption occurs at 2.0 μm, which is strongest in the calcite spectrum and weakest in epidote.

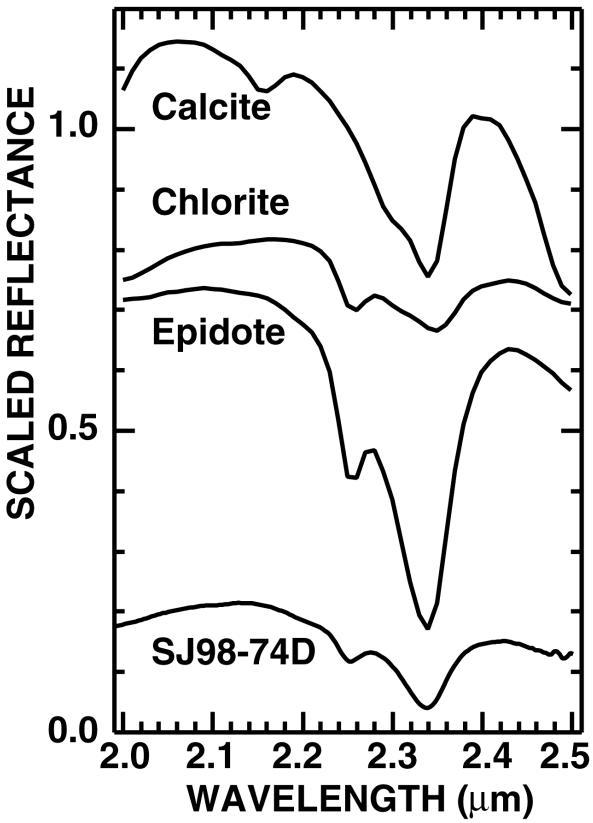

Figure 1. Infrared spectra of calcite, chlorite and epidote, along with spectrum of field sample SJ98-74D, a rock containing all three in a fine-grained matrix. The intimate mixture produces a spectrum exhibiting features of all three components.

This last absorption is not useful for terrestrial remote sensing studies because it conflicts with atmospheric water vapor. The 2.1- μm calcite absorption, in turn, cannot be used because it lies very close to a clay mineral feature centered at 2.2 μm. Since all of the remotely-sensed spectra in this study (and most AVIRIS studies) are of mixtures of a variety of materials, the discrimination method must be highly robust. While the 2.26-μm absorption seen in the chlorite and epidote spectra is sufficient to separate them from calcite when comparing pure samples in the laboratory, a further complication arises in the field. This is illustrated by the fourth spectrum in Figure 1, that of a rock sample acquired during preliminary field-checking of the classified AVIRIS data. Laboratory analysis shows sample SJ98-74D to be a fine-grained mixture of 44.58% epidote, 10.98% chlorite, and 6.73% calcite in a propylitic matrix containing other, infrared-inactive minerals. Normalized for weight, the spectral contributions of the three spectrally active minerals come to approximately 70% epidote, 20% chlorite, and 10% calcite. Since it is a fine-grained mixture, its spectrum is not a simple linear combination of its pure components. The infrared spectrum of this ground-truth sample has the same band center as calcite, despite its low calcite content. The overall band shape, width and position correlate strongly with all three of the pure endmember spectra. Given current signal-to-noise ratios, combined with other potential sources of error, a classification algorithm based only on the pure endmember information might easily misidentify the sample. Divulging the relative abundance of calcite, and thus acid-buffering potential, throughout the AVIRIS scenes is not therefore a matter of comparing single-channel intensity levels, ratios of band depths, nor even continuum-removed, area-weighted correlation coefficients of pure endmembers. Two main approaches may lend themselves to the solution of this problem: the first is the mathematically elegant, computationally expensive

quantitative unmixing approach based on optical constants (Hapke, 1993; Mustard and Sunshine, 1999); and the second is the less elegant empirical approach of comparing spectra of an assortment of fine-grained laboratory mixtures. Given the present limitations of modern microprocessors, this study utilizes the latter approach.

3. DETAILS OF EMPIRICAL APPROACH

3.1 Tetracorder Algorithm

The USGS Tetracorder Expert System (Clark *et al*. 2001, Clark and Swayze 1995, Clark *et al*. 1990) has been described fully elsewhere; such a description is beyond the scope of this paper and the reader is advised to consult the references given. The heart of the method is the comparison of continuum-removed absorption bands of spectra kept in a reference library, to those of an observed spectrum. The Tetracorder Algorithm can be trained to compare sets of diagnostic bands for a given material, and even exclude materials from consideration based on the presence or absence of certain bands . Each band under consideration is normalized against its continuum and then scaled by a multiplicative constant so that its depth matches that of the corresponding reference band. Least-squares correlation coefficients are calculated and weighted according to the area under the curve and optional user-defined weights. Sets of bands for specific materials are compared based on a prescribed set of rules. An identification is issued based on application of these rules to the calculated values. For imaging spectroscopy applications, an image is generated for each material under consideration, with the intensity of each pixel corresponding to the product of correlation coefficient and absorption band depth; this roughly scales with abundance (Clark *et al*., 1990). The images of relevant materials are then assembled into a classified image.

3.2 Laboratory and field samples

For this study, the reference library (Tetracorder v3.6a2) of over 400 minerals, vegetation species, snow cover types and manmade materials was augmented with laboratory spectra of mixtures of calcite, epidote and chlorite. Figure 2 is a ternary diagram indicating the pure endmembers, mixture proportions, and a number of rock samples acquired in the field and used for testing. A set of field samples collected under a different portion of the watershed study was analyzed for composition using point counts of mineral grains to determine relative weight percents of calcite, epidote and chlorite. Due to expense, only two samples collected from known regions previously misidentified as calcite but actually containing little to no calcite could be analyzed in this manner. Most of the samples cluster in one region of the diagram, indicating a tendency toward such mixtures. Whether this is caused by selection effects during field sampling or, as is quite likely, accurately reflects the composition of the study region, is of little consequence to this study, because in any case a robust discrimination algorithm requires a consistent spread of compositions throughout the ternary diagram. For this reason as well as the presence of other mineral phases in the samples, the use of laboratory mixtures was deemed to give a more accurate reference set. Pure samples of each mineral were ground and wet-sieved using methanol. The 75–150-μm size fraction was found to closely match the band depths of pure inclusions of calcite, epidote and chlorite in the field samples. This fact conveniently eliminated sources of error due to differences in grain size between minerals in the mixtures. A set of powdered mixtures was prepared from the pure endmembers, in ratios allowing each of the three minerals commensurate representation in relation to the other two, as either major, equal, or minor proportions. These proportions are indicated on the ternary diagram by the letters B through N, and given numerically in Table I. Sample F (80% epidote, 10% each of calcite and chlorite) was omitted because the strong epidote signal rapidly overwhelms the other two minerals as epidote concentration increases. This is borne out by examination of continuum-removed spectra of mixture CEC-G and samples SJ98-74D and IDB6597. For realistic instrument noise levels, these mixtures will inevitably be classified as high in epidote and low in calcite.

Although it would seem that the 2.26 μm band in the spectrum of sample SJ98-74D could be used to rule out a pure calcite identification, in practice the quality of remotely sensed spectra are presently too noisy for this band to be reliable in automated applications. If all spectra in the scene were of similar quality to the laboratory data shown above, the solution would be trivial. However, due to their differing shapes, the quality of a least-squares match between SJ98-74D and each of the three endmembers is roughly the same for each, with typical noise levels sufficient to skew the results in favor of the wrong endmember. Furthermore, this study aims to determine the

distribution of calcite in mixtures as well. With the full suite of mixtures B through N listed in Table I, such a misidentification becomes much less likely.

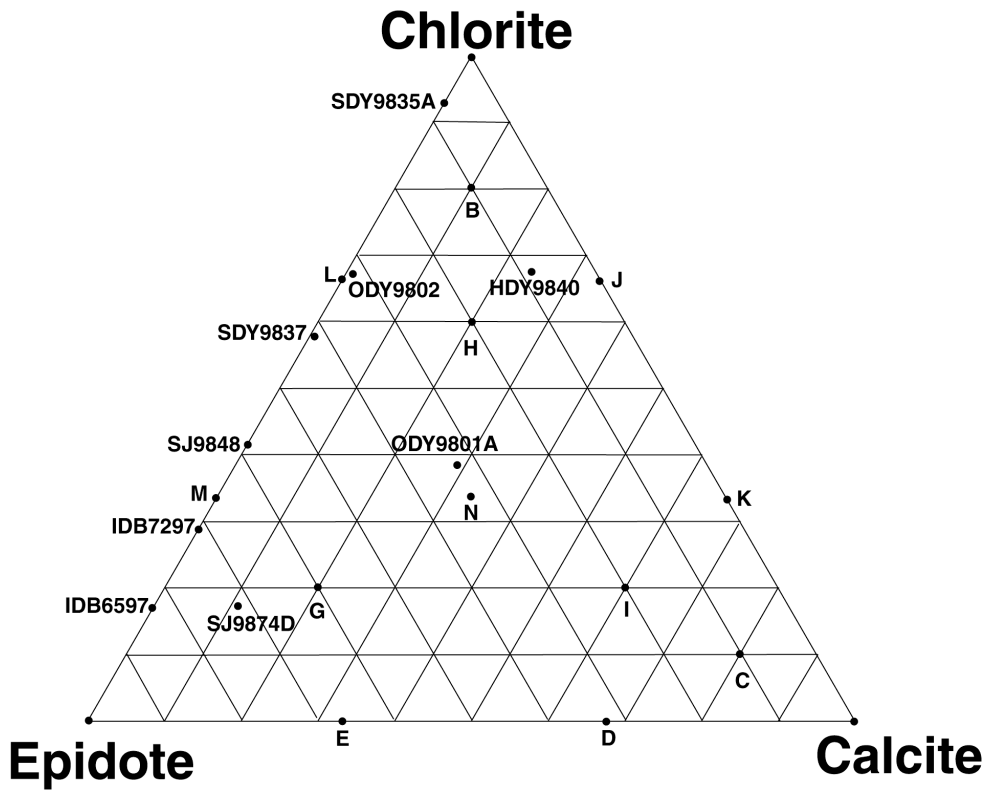

Figure 2. Ternary diagram indicating proportions of calcite, epidote and chlorite in each of the laboratory mixtures and several rock samples collected in the field. Vertices are 100% endmember; each line denotes a ten percent change in concentration.

Table I. Numeric values of proportions of calcite, epidote and chlorite used in mixtures.

Sample ID	% Calcite	% Epidote	% Chlorite
Calcite (GDS-304)	100		
Epidote (GDS-301)		100	
Chlorite (GDS-307)			100
CEC-B (GDS-308)	10	10	80
CEC-C (GDS-309)	80	10	10
CEC-D (GDS-310)	67	33	
CEC-E (GDS-311)	33	67	
CEC-G (GDS-312)	20	60	20
CEC-H (GDS-313)	20	20	60
CEC-I (GDS-314)	60	20	20
CEC-J (GDS-315)	67		33
CEC-K (GDS-316)	33		67
CEC-L (GDS-317)		33	67
CEC-M (GDS-318)		67	33
CEC-N (GDS-319)	34	33	33

All laboratory spectra were acquired using an Analytical Spectral Devices ASD-6015-7 Field Spectrometer with a quartz halogen light source and Spectralon reference standard. The spectral sampling of this instrument is 2 nm while the resolution is 11 nm (Goetz *et al*., 1998). Wavelength calibration was performed using praseodymium-doped Corning Glass along with mylar plastic sheeting as transmission standards. The spectrometer was programmed to average 60 measurements, each having a one second integration time, together per spectrum; 25 such spectra were averaged to produce each reference spectrum, for a total integration time of 1800 seconds apiece. All spectra were corrected to absolute reflectance.

The reference spectra for the three endmembers and the twelve mixtures are shown in Figure 3. The depth of the primary band at 2.34 μm scales nonlinearly with composition; the resultant spectra are most sensitive to epidote. Note that the 2.26-μm secondary band is evident in all of the mixture spectra, including those (C, D, and K) dominated by calcite. The effects of small amounts of calcite on the overall band shape are more subtle, yet with 21 separate channels in the AVIRIS spectra of this band complex, the least-squares correlation coefficients differ sufficiently for the Tetracorder algorithm to distinguish between them.

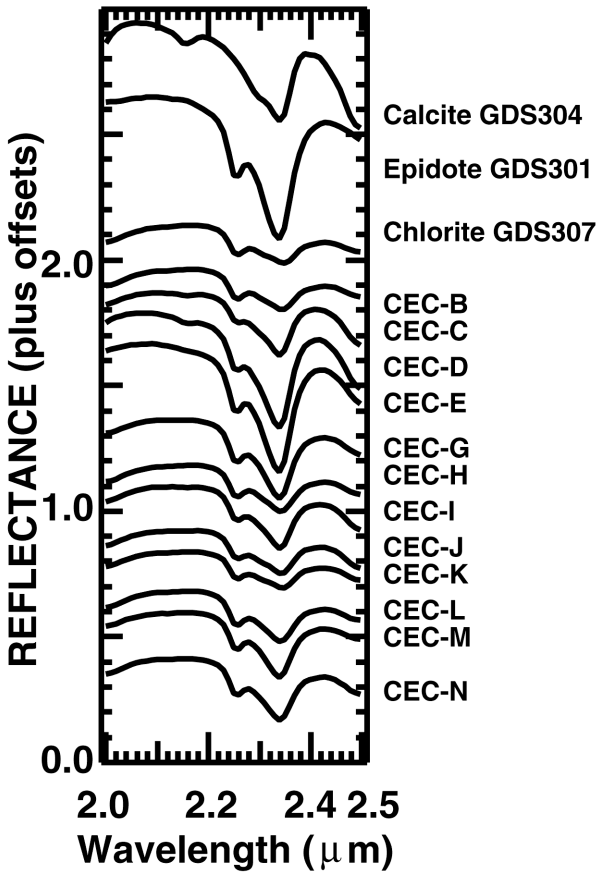

Figure 3. The 2.3-μm feature complex of calcite, epidote, chlorite and the twelve mixtures used to train the Tetracorder algorithm.

3.3 Tetracorder Processing

Each of the mixture spectra were added to the USGS Denver Spectroscopy Laboratory Tetracorder 3.6a2 reference library. The default continuum-removal approach was to fit a straight line to the reflectance continuum using the two continuum points on either side of the absorption band (Clark and Roush, 1984) and divide the spectrum by this fitted continuum line. In order to compare continuum-removed features, tie points were established at the edges of the primary band (at 2.18 and 2.42 μm) and also, separately, for the secondary band (2.21 and 2.28 μm) for each of the mixtures. The tie points for continuum removal were slightly different for each of the pure endmembers, leading to a better continuum-removed correlation coefficient for the pure cases.

The algorithm was tested first using the laboratory mixtures as the "observed" test spectra. All mixtures were properly categorized. The 2.15-μm calcite feature was not used in either the testing or analysis phases. The method was then tested on the field samples. There were problems classifying certain of the field samples due to the presence of a fourth spectrally active component, sericite, in several specimens. Sericite is a fine-grained form of muscovite which has a strong diagnostic feature at 2.2 μm and two weaker features at 2.35 and 2.45 μm which overlap the 2.3-μm wings of calcite, epidote and chlorite, complicating their identification. This is addressed in section 4.3. The two specimens collected during AVIRIS field-checking (SJ98-74D and SJ98-48) had previously been identified as calcite but were correctly identified as mixtures using the improved reference library. These samples contained no sericite. Extracted pixels from AVIRIS scenes corresponding to calcite-epidote-chlorite mixtures were the used as test spectra, and correctly identified as mixtures dominated in turn by each of the three. Pure samples of the endmembers, and library specimens of other epidote, calcite and chlorite samples were also correctly identified with the improved reference spectra. The new approach also correctly identified limestones.

The next step was application to the AVIRIS Animas Watershed flightlines. These two flight lines were acquired on June 18, 1996 at 9:30 AM and cover the region from Durango, Colorado to the headwaters of the Animas River at Animas Forks, Colorado. The study area is bounded by national forest on the east and west sides, and includes the town of Silverton and all of the Silverton Caldera. The full dataset and its analysis are described elsewhere (Dalton *et al*., 2000, 2001); this paper is concerned specifically with the calcite-epidote-chlorite results, which are discussed below.

4. Results

4.1 Regional Context

The USGS Tetracorder Algorithm was able to successfully utilize the updated reference library to distinguish between the calcite, epidote and chlorite endmembers. Most importantly, nearly pure calcites such as limestone were easily differentiated from mixtures of calcite, epidote and chlorite. While AVIRIS pixels were separated into bins corresponding to each of the mixtures, it must be recognized that such fine division is in fact splitting hairs, due to inherent noise and the contributions of other materials in the scene.

The final images produced by the algorithm were grouped together into images reflecting the surface composition in a more general fashion. Referring to the ternary diagram of Figure 2, it is clear that many possible compositions would fall into the category of mixture CEC-N (equal parts calcite, epidote and chlorite) and many possible mixtures would fall into category CEC-D (mostly calcite, with epidote but no chlorite.) The georeferenced, orthorectified image in Figure 4 reflects an intuitive grouping of these materials. The color key shows each endmember having a certain primary color (yellow for calcite, blue for epidote, red for chlorite) and the mixtures represented by secondary colors. Thus, yellow-green represents a mixture of predominantly calcite but also containing epidote, similar to the region around sample mixture CEC-D in Figure 2; dark green is primarily calcite but contains both epidote and chlorite, as with mixtures CEC-I and CEC-C and the region surrounding them; blue-green is epidote with some calcite, as with CEC-E; and so forth.

Examining Figure 4, the regional context of the study becomes clearer. The town of Silverton is situated within the caldera and appears at the top center of the image. The confluence of the Animas River with Mineral Creek lies just below the town, and the river cuts through the center of the image. Sultan Mountain lies southwest of the confluence; Molas Lake, Little Molas Lake, and Andrews Lake are to the west of the river toward the middle of the image. As the river leaves the caldera just south of the town, it cuts through the sedimentary formations containing abundant limestones. The yellow outcrop of limestone in the lower left of the image is near the aptly-named Lime Creek, which flows into the Animas and contributes to the buffering of acidic waters introduced upstream by Mineral Creek. Limestones are also evident in road cuts paralleling the river just east of Sultan Mountain. The propylitic alteration zones in the upper right-hand corner of the image, however, exhibit a patterning which is due to the varying calcite, epidote and chlorite concentrations in the altered host rock. Preliminary analyses using Tetracorder v3.4a8 (Dalton *et al*., 1998) classified much of this material as calcite.

4.2 Discrimination of Calcite-Epidote-Chlorite Mixtures

The propylitically altered zone from Figure 4 is enlarged in Figure 5 to show more details of the differentiated mixtures. The key is the same as for Figure 4. The astute reader will notice that there are no chlorite-dominated mixtures in the key other than chlorite with muscovite. During processing, it was found that few AVIRIS pixels gave a good match to a chlorite-dominated mixture. Pixels were generally dominated by either epidote or calcite. Referring to the ternary diagram in Figure 2, it is seen that few field samples from the Animas River Watershed and Silverton Caldera were dominated by chlorite. Laboratory analyses showed that most of these also contained sericite. The Tetracorder analysis found essentially the same thing: although there are some regions where chlorite does dominate the spectral signature, most areas lacking in epidote and calcite contained sericite as well. A more detailed discussion follows in section 4.3. The categories of mixtures CEC-B and CEC-C were found to be superfluous as well; along with CEC-F, the mixtures containing 80% of any one endmember gave similar correlations to the pure endmembers and were therefore not considered in the final analyses. As chlorite and

muscovite had already been encountered together in a different location (Swayze 1997), a chlorite-muscovite mixture was already in the USGS Tetracorder (v3.4a8) reference library (Dalton, 1998).

Four primarily northwest-southeast trending zones of exposed propylitic alteration are visible in Figure 5. The ridge of Hazelton Mountain in the upper right corner is highlighted in a profusion of light and dark blue, yellow-green and

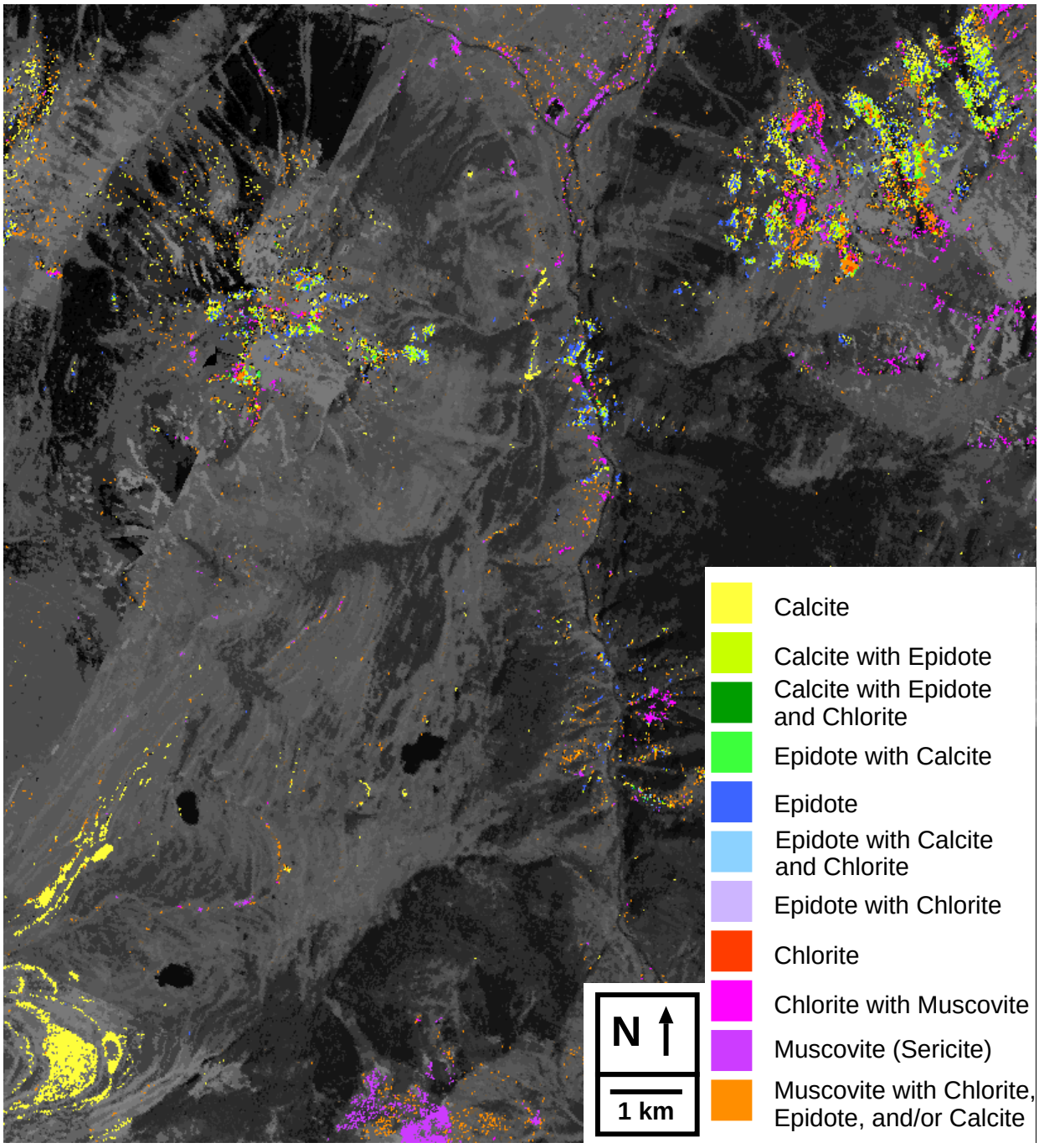

Figure 4. Georeferenced image of a portion of the Animas River Watershed study area. Tetracorder results are shown in color. The town of Silverton, Colorado is near the top center; the Animas River bisects the image vertically. This image has been engineering-corrected for roll, pitch, yaw, forward velocity, and smile, as well as orthorectified against a digital elevation model to remove topographic distortions.

yellow, evidence of mixtures of epidote and calcite. Although few pixels exactly matched the equal- parts mixture (CEC-N, 33% each), the dark green and light blue pixels illustrate areas containing all three minerals. An outcrop of predominantly chlorite (red) in the lower left corner lies on Kendall Mountain. The intermediate slopes contain a combination of all of these, along with orange pixels denoting the presence of all four minerals. In these orange pixels, no single mineral dominates the spectrum strongly enough to be realistically selected as the primary mineral. Within the limits of current technology, such pixels cannot yet be further constrained. An additional source of uncertainty arises from the presence of sericite around the edges of the zone. Regions identified as pure sericite (muscovite) are shown in purple while the chlorite-sericite mixture is shown in pink. These give some idea of how the sericite grades into the rest of the propylitic assemblages. Fortunately, there appears to be a steady and gradual shift from calcite-dominated to sericite-dominated spectra. Were the sericite randomly distributed throughout the zones, this would be cause for concern.

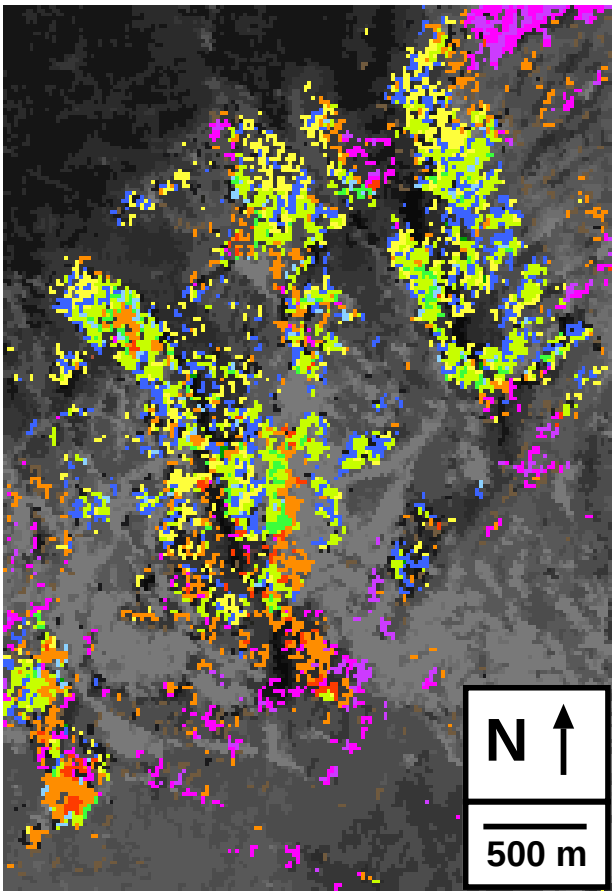

Figure 5. Enlargement of a portion of Figure 4 showing calcite, epidote, chlorite and muscovite mixtures in the Silverton Caldera. Woodchuck Basin lies right of center, between the ridges of Mount Hazelton (top right) and Mount Kendall (bottom center). Key is the same as in Figure 4.

The heterogeneous mix of pixels dominated by calcite, epidote and chlorite are indicative of the actual variations of concentration in the host rock. These variations result from the initial composition of the rock, variations in severity of propylitic alteration, and subsequent weathering. Although these specific slopes were not field-checked, earlier traverses of similar propylitic alteration zones in the watershed revealed exactly this pattern. The stronger spectral signal of epidote probably results in a slight overestimation of its abundance in these images. Likewise, the weaker signal of chlorite has probably caused its distribution to be slightly underestimated. However, these images represent a significant improvement over previous methods in deducing the distribution of calcite in the watershed, and will result in improved determination of stream buffering capacity from naturally occurring deposits.

4.3. The Muscovite Problem

Care should be applied when interpreting these results. As noted earlier, all chlorites in this region were well-represented by ripidolite. This is likely not the case at all sites outside of this study area. In addition, it must be stressed that the presence of sericite in propylitic alteration zones was not taken fully into account in this study. Because muscovites have a strong diagnostic absorption feature at 2.2 μm, and weaker absorptions at 2.35 and 2.45 μm, they interfere spectrally with the absorptions of calcite, epidote and chlorite. In the present study, this results in uncertainty in the absolute abundances of the minerals of interest. For locations evidencing the muscovite bands, relative concentrations of the three could not be established, and the Tetracorder algorithm was instructed to differentiate these into three categories. The easiest of course was muscovite only (purple in the key to Figure 4). Where the chlorite signature was seen together with muscovite, pixels were categorized as chlorite with muscovite (pink.) It is interesting to note that there was no apparent evidence for sericite alone with either calcite or epidote. In

the case of mixed pixels of epidote, calcite and/or chlorite, together with the muscovite signature at 2.2 μm, nothing further could be determined about the composition and these are the orange pixels in Figures 4 and 5.

A ready solution to this problem could be to conduct a similar study to this one, using laboratory mixtures of four endmembers instead of three. Due to financial and timing constraints, this was not possible within the current study. In planning for such work, the obvious question of whether a fifth, sixth and seventh such endmember could crop up was investigated. Examination of the AVIRIS spectra, laboratory spectra, field samples and laboratory mixtures indicates that there are no other spectrally active materials in the study area in this region of the spectrum which do not have other diagnostic features already being used by the Tetracorder system. Once appropriate mixtures of muscovites have been added to the reference library, the algorithm should be able to distinguish the remaining four-endmember (orange) pixels and further constrain the abundance of calcite and chlorite in the watershed.

5. Conclusion

The application of the USGS Tetracorder algorithm to the Animas River Watershed study demonstrates the ability of rule-based expert systems to differentiate between spectrally similar materials using comparisons of least-squares correlation coefficients derived from a reference library to those of the observed spectral data set. Including a set of spectra representing mixtures of the discrete endmembers calcite, epidote and chlorite was an essentially simple adjustment which enabled accurate discrimination between mineral mixtures in the host rock. The approach could be refined by the addition of muscovite-calcite-epidote-chlorite mixtures to the reference library. Researchers applying these results to other regions should first ensure that ripidolite is representative of the chlorites in their region of interest, or else adapt their reference library with local chlorites. This approach should prove useful in identifying other spectrally similar materials. These results will be useful to land managers wishing to constrain problems of acidic drainage in the Animas River Watershed, as well as to remote-sensing scientists with similar applications.

REFERENCES

Bigham, J.M., U. Schwertmann, S.J. Traina, R.L. Winland, and M. Wolf, Schwertmannite and the chemical modeling of iron in acid sulfate waters, *Geochimica et Cosmochimica Acta*, **60:**2111-2121, 1996.

Boardman, J.W., Automated spectral unmixing of AVIRIS data using convex geometry concepts, *Summaries of the 4th Annual JPL Airborne Geoscience Workshop*, JPL Publ. 93-26, **1**, Pasadena CA 1993.

Bove, D.J., M.A. Mast, W.G. Wright, P.L. Verplanck, G.P. Meeker, and D.B. Yager, Geologic control on acidic and metal-rich waters in the southeast Red Mountains area, near Silverton, Colorado, *Proceedings of the 5th International Conference on Acid Rock Drainage*, Denver CO 2000.

Church, S.E., D.L. Fey, and R. Blair, Pre-mining bed sediment geochemical baseline in the Animas River Watershed, southwestern Colorado, *Proceedings of the 5th International Conference on Acid Rock Drainage*, Denver CO 2000.

Clark, R.N. and T.L. Roush, Reflectance spectroscopy: Quantitative analysis techniques for remote sensing applications, *J. Geophys. Res.*, 89:6329-6340, 1984.

Clark, R.N., A.J. Gallagher, and G.A.S. Swayze, Material absorption band depth mapping of imaging spectrometer data using complete band shape least-squares fit with library reference spectra, *Proceedings of the 2nd annual JPL Airborne/Visible Imaging Spectrometer (AVIRIS) Workshop*, JPL Publ. 90-54, Pasadena, CA 1990.

Clark, R.N. and G.A.S. Swayze, Automated spectral analysis: mapping minerals, amorphous materials, environmental materials, vegetation, water, ice and snow, and other materials: The USGS Tricorder Algorithm, *Lunar and Planetary Science XXVI*, pp. 255-256, 1995.

Clark, R.N., G.A. Swayze, T.V.V. King, K.E. Livo, J.B. Dalton, and R.F. Kokaly, Expert system features identification rules for reflectance (and emittance) spectroscopy analysis I: Visible to near-infrared detection of minerals, organics, vegetation, water, amorphous and other materials, *J. Geophys. Res.*, 2001.

Dalton, J.B., T.V.V. King, D.J. Bove, R.F. Kokaly, R.N. Clark, J.S. Vance, and G.A.S. Swayze, Mapping of acid-generating and acid-buffering minerals in the Animas watershed by AVIRIS spectroscopy, *Summaries of the 7th Annual JPL Airborne Earth Science Workshop*, JPL Publ. 97-21, pp. 79-83, 1998.

Dalton, J.B., T.V.V. King, D.J. Bove, R.F. Kokaly, R.N. Clark, J.S. Vance, and G.A.S. Swayze, Distribution of acid-generating and acid-buffering minerals in the Animas River watershed by AVIRIS spectroscopy, *Proceedings of the 5th International Conference on Acid Rock Drainage*, Denver CO 2000.

Dalton, J.B., D.J. Bove, T.V.V. King, C.A. Mladinich, R.N. Clark, B. Rockwell, G.A.S. Swayze, R.F. Kokaly, K.E. Livo, J.S. Vance and S.E. Church, Remote Sensing Characterization of the Animas River Watershed by AVIRIS Imaging Spectroscopy,*to be published in U.S. Geological Survey Open File Report*, in technical review, 2001.

DesBorough, G.A., P.H. Briggs, and N. Mazza, Chemical and mineralogical characteristics and acid-neutralizing potential of fresh and altered rocks and soils of the Boulder River Headwaters in Basin and Cataract Creeks of northern Jefferson County, Montana, *U.S. Geological Survey Open File Report 98-40*, 1998.

Eastwood, M.L., R.O. Green, C.M. Sarture, B.J. Chippendale, C.J. Chovit, J.A. Faust, D.L. Johnson, S.P. Monacos, and J.J. Raney, Recent improvements to the AVIRIS Sensor: Flight Season 2000, *Proceedings of the 9th JPL Airborne Earth Science Workshop*, JPL Publ. 00-18 Pasadena, CA 2000.

Fleischer, M. and J.A. Mandarino, *Glossary of Mineral Species*, Mineralogical Record, Inc. Tucson AZ 1995.

Goetz, A.F., K.B. Heidebrecht, B. Kindel, and J.W. Boardman, Using ground spectral irradiance for model correction of AVIRIS data, *Summaries of the 7th Annual JPL Airborne Earth Science Workshop*, JPL Publ. 97-21, pp. 159-168, 1998.

Hapke, B., *Theory of reflectance and emittance spectroscopy*, Cambridge University Press, Cambridge, 1993.

Hunt, G.R. and J.W. Salisbury, Visible and near-infrared spectra of minerals and rocks: I. Silicate Minerals, *Modern Geology* **1**:283-300, 1970.

King, T.V.V. and R.N. Clark, Spectral characteristics of chlorites and Mg-serpentines using high-resolution reflectance spectroscopy, *J. Geophys. Res.* **13**:13997-14008, 1989.

Klein, C. and C.S. Hurlbut, *Manual of Mineralogy*, John Wiley and Sons, New York, 1993.

Kokaly, R.F., R.N. Clark, and K.E. Livo, Mapping the biology and mineralogy of Yellowstone National Park using imaging spectroscopy, *Summaries of the 3rd Annual JPL Airborne Geoscience Workshop*, JPL Publ. 97-21, **1**, Pasadena CA 1997

Kruse, F.A., A.B. Lekhoff, and J.B. Dietz, Expert system-based mineral mapping in northern Death Valley, California/Nevada, using the Airborne Visible/Infrared Imaging Spectrometer (AVIRIS), *Remote Sensing Environ.*, 44, pp. 309-335, 1993.

Lipman, P.W., T.A. Steven, R.G. Luedke, and W.S. Burbank, Revised volcanic history of the San Juan, Uncompahgre, Silverton, and Lake City calderas in the western San Juan Mountains, Colorado, *U.S. Geological Survey Journal of Research* **1**:627-642, 1973.

Mast, M.A., P.L. Verplanck, D.B. Yager, W.G. Wright, and D.J. Bove, Natural sources of metals to surface waters in the Upper Animas River Watershed, Colorado, *Proceedings of the 5th International Conference on Acid Rock Drainage*, Denver CO 2000.

Mustard, J.F. and J.M. Sunshine, Spectral Analysis for Earth Science: Investigations Using Remote Sensing Data, in *Remote Sensing for the Earth Sciences: Manual of Remote Sensing*, Ed. A.N. Rencz, John Wiley & Sons, New York, 1999.

Nimick, D.A. and P. von Guerard, Science for Watershed Decisions on Abandoned Mine Lands: Review of Preliminary Results, *U.S. Geological Survey Open File Report 98-297*, 1998.

Soha, J.M., A.R. Gillespie, M.J. Abrams, and D.P. Madura, Computer Techniques for Geological Applications, Caltech/JPL Conference on Image Processing Technology, Data Sources and Software for Commercial And Scientific Applications, JPL SP 43-30, pp. 4.1-4.21, Pasadena CA, 1976.

Swayze, G.A.S., The hydrothermal and structural history of the Cuprite Mining District, southwestern Nevada: an integrated geological and geophysical approach, Ph.D. dissertation, University of Colorado, Boulder, 1997.